IEEE Access
Multidisciplinary | Rapid Review | Open Access Journal

Received January 17, 2021, accepted January 27, 2021, date of publication February 5, 2021, date of current version February 12, 2021.

Digital Object Identifier 10.1109/ACCESS.2021.3057386

An Improved Deadbeat Control Strategy Based on Repetitive Prediction Against Grid Frequency Fluctuation for Active Power Filter

JIKAI CHEN, (Member, IEEE), HUI SHAO, AND CHUANG LIU, (Member, IEEE)
School of Electrical Engineering, Northeast Electric Power University, Jilin City 132012, China

Corresponding author: Jikai Chen (chenjikai@neepu.edu.cn)

This work was supported in part by the National Natural Science Foundation of China (NSFC) under Grant 52077030, in part by the Department of Science and Technology of Jilin Province under Grant 20190701014GH, and in part by the Jilin Province Development and Reform Commission under Grant 2019C058-6.

ABSTRACT In order to improve the harmonic compensation performance of active power filter (APF) in distribution network, based on deadbeat control theory, the command current prediction algorithm and current tracking control strategy are optimized in this article. Firstly, the command current repetitive prediction in abc coordinate system is transferred to dq for improving its accuracy in lead compensation, and the equivalent for fractional delay beat is achieved by Lagrange Interpolation Polynomial to solve the problem of inaccurate prediction caused by grid frequency fluctuation. Then, considering the inherent half-sampling-period delay of sinusoidal PWM (SPWM), an improved deadbeat control strategy for current tracking is proposed by estimating the output current of next sampling period. Because the output current in next sampling period is replaced by that in current sampling period with traditional deadbeat control strategy, this estimation could make up for the defect of low control precision caused by that replacement. After that, adding error repetitive correction into the improved deadbeat control channel to reduce the periodic tracking error of output current. Finally, the stability and accuracy of the improved control system are analyzed theoretically, and its feasibility and effectiveness are verified by the simulation and hardware-in-the-loop (HIL) experiments.

INDEX TERMS Deadbeat control, frequency fluctuation, harmonic compensation, Lagrange interpolation polynomial, error repetitive correction.

I. INTRODUCTION

With an increasing of nonlinear loads and power electronic converters in the grid, power quality problem has become a vital issue in the current research on intelligent distribution network [1], [2]. As the one of power quality regulators, APF can not only realize the harmonic current suppression but also complete the real time adjustment of reactive power [3], [4].

Numerous researches have shown that the harmonic compensation effectiveness of APF mainly depends on the control performance of the inner current loop [5], [6]. Many current control strategies for the APF have been proposed [7].

Due to the simple control structure and fast response, hysteresis current controller is widely applied to derive switching signals by comparing a fixed hysteresis band with the current tracking error in harmonic compensation [8], [9]. However a varying modulation frequency is inducted into APF, which results in the difficulty in designing the output filters for suppression of unwanted resonance. PI controller is used in multiple synchronous rotation coordinate systems by using PLL, so that the specific harmonic components of load current can be converted into DC variables in control process. Therefore, the DC variables can be tracked without static error by PI controller [10], [11]. Nevertheless, the flexibility of PI control is unsatisfactory, and it is limited to apply in some load with the special harmonics. Based on internal model principle, repetitive control can track periodic signal without static error, which could make the system have a satisfactory steady-state tracking performance [12], [13], [14]. Because the high gain at the integral multiple harmonic frequencies is obtained by time delay, a poor dynamic-state response becomes an inevitable defect.

The associate editor coordinating the review of this manuscript and approving it for publication was Amjad Anvari-Moghaddam.

As a digital control method with high efficiency, deadbeat control is widely applied in the current inner loop of APF because of its clear mathematical characterization, high tracking accuracy and rapid dynamic response [15], [16].

Currently, the researches for deadbeat control mainly focus on the optimization of command current prediction algorithm and command current tracking control strategy. Regarding the command current prediction, an extrapolation prediction algorithm is adopted, which directly takes the command current in the current sampling period as the prediction value [17]. Although the calculation speed is fast without real prediction, the extrapolation prediction could cause the increase of prediction error and decrease of dynamic control accuracy, especially when the load fluctuates frequently. The corresponding command in previous power grid cycle is used as the prediction result, it is concise in algorithm structure and good in static accuracy [18]. However, the dynamic prediction effect is poor because of the one-power-cycle prediction delay. Repetitive control is introduced to the calculation for command current prediction [19], [20]. This prediction method can obtain the good static and dynamic accuracy, but the prediction value is to be corrected only once in one power cycle. Moreover, the influence of grid frequency fluctuation on the prediction accuracy is not considered in this algorithm.

For the studies of command current tracking control strategy, reference [21] introduces an average coefficient in the control channel at the cost of sacrificing the current tracking accuracy, so as to ensure the stability and dynamic performance of the APF control system. Reference [22] proposes a current tracking error elimination method, when the command current changes significantly, a compensation value is added in the output voltage command to offset the tracking error. However, the number of offsetting beats is limited and the control algorithm is relatively complex. References [23], [24] propose a deadbeat control strategy without tracking error, which make the closed-loop transfer function of the current inner loop to 1. But this method supposes that the output voltage is absolutely equal to the command voltage, which declines control accuracy obviously. In [25], in order to enhance the steady-state harmonic compensation performance, repetitive control is connected in series to deadbeat control channel, but the delay of repetitive control also reduces the dynamic response speed. In [26], [27], repetitive control is paralleled to the deadbeat control channel, this way could raise the dynamic response speed of APF. However, the inherent delay of SPWM is not considered in the control system, resulting in a deviation between the theoretical model and the actual situation.

Regarding problems above, deadbeat control in current inner loop of APF is taken as the research object in this article. On the one hand, in order to improve the prediction accuracy of command current, an optimized command current prediction algorithm is proposed in Section III, which realizes the quick correction of current prediction value and improves the anti-interference ability of grid frequency fluctuation. On the other hand, in Section IV, for the problem of current tracking control accuracy in traditional deadbeat control strategy, the output current of APF in the next sampling period is estimated, which is based on the half-sampling-period delay caused by SPWM. Furthermore, the error repetitive correction is added into the improved deadbeat channel. In Section V, effectiveness of the proposed method is verified by simulation and experiment. The rest of this article is arranged as follows: Section II analyzes the APF equivalent model and principle of deadbeat control, Section VI exhibits the conclusion in the end.

II. EQUIVALENT MODEL OF THREE-PHASE APF AND DEADBEAT CONTROL PRINCIPLE

A. EQUIVALENT MATHEMATICAL MODEL OF THREE-PHASE APF

To avoid harmonic pollution in grid-side current, APF derives corresponding current to eliminate the harmonic components of load [28]. Three-phase APF topology and the overall control structure are shown in Fig. 1, where u_s is grid voltage, u_o is the output voltage and i_c is the output current of APF, i_s is grid-side current and i_L is the nonlinear load current.

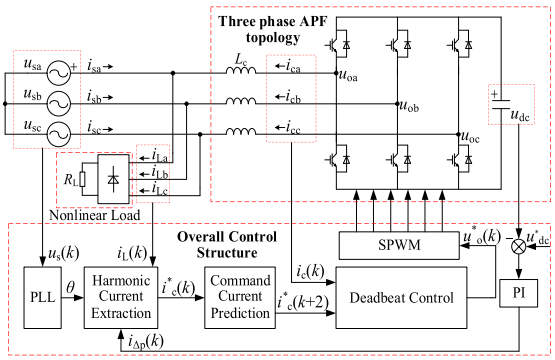

FIGURE 1. Three-phase APF topology and overall control structure.

Ignoring the parasitic resistance of inductor, with the reference direction of each variable in Fig. 1, the APF equivalent mathematical model in time domain described by differential equation is:

$$u_{ox} = u_{sx} + L_c \frac{\mathrm{d}i_{cx}}{\mathrm{d}t} x = \mathrm{a, b, c} \tag{1}$$

By discretizing (1), (2) can be gotten:

$$i_{cx}(k+1) = i_{cx}(k) + \frac{T_s}{L_c}\left[u_{ox}(k) - u_{sx}(k)\right] \tag{2}$$

where T_s is sampling period of the controller (for simplicity, the subscript x will be omitted in the following analysis).

B. PRINCIPLE OF DEADBEAT CONTROL STRATEGY

Ideally, if the command current can be tracked in a sampling period, the expected harmonic compensation performance can be sustained, namely:

$$i_c(k+1) = i_c^*(k) \tag{3}$$

Introducing (3) into (2), the corresponding command voltage (modulation signal) $u_o^*(k)$ will be expressed as (4).

$$u_o^*(k) = \frac{L_c}{T_s}\left[i_c^*(k) - i_c(k)\right] + u_s(k) \tag{4}$$

Operation time of $u_o^*(k)$ is the current sampling period: $kT_s - (k+1)T_s$.

In order to avoid multiple intersection between modulation signal and carrier signal in a sampling period, and considering the time consumed for sampling and calculation during digital control process, the modulation signal is usually delayed to be loaded in the next sampling period. That is to say, $u_o^*(k)$ will be loaded at the moment of $(k+1)T_s$. Therefore, the tracking target of output current $i_c(k+2)$ sampled at $(k+2)T_s$ is $i_c^*(k)$, which is corresponding to sampling current at kT_s. The command voltage loaded at $(k+1)T_s$ is obtained by (5).

$$u_o^*(k+1) = \frac{L_c}{T_s}\left[i_c^*(k) - i_c(k)\right] + u_s(k) \tag{5}$$

The operation time of $u_o^*(k+1)$ is the next sampling period: $(k+1)T_s - (k+2)T_s$.

It can be inferred from (5) that the actual output current of APF will lag behind the corresponding command current for two sampling periods. Therefore, in traditional deadbeat control strategy, command current should be predicted two sampling periods in advance ($i_c^*(k+2)$ should be predicted in $kT_s - (k+1)T_s$). The purpose of this prediction is to ensure that tracked target of the output current in current period is the command current in the same period. The practical command voltage loaded at $(k+1)T_s$ will be calculated from (6).

$$u_o^*(k+1) = \frac{L_c}{T_s}\left[i_c^*(k+2) - i_c(k)\right] + u_s(k) \tag{6}$$

Based on the discussion above, time sequence of traditional deadbeat control is shown in Fig. 2.

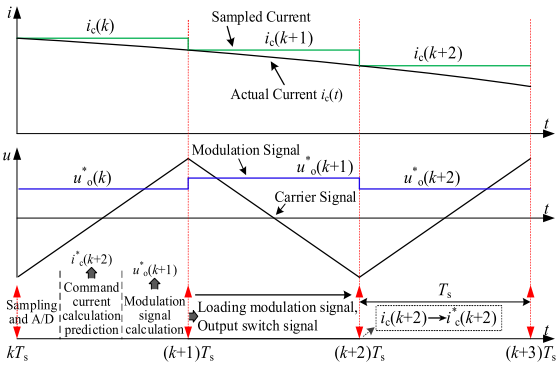

FIGURE 2. Time sequence of traditional deadbeat control.

C. OVERALL CONTROL STRUCTURE

In Fig. 1, the overall control structure for APF is composed of harmonic current extraction, command current prediction, deadbeat control strategy in current inner loop and DC side voltage controller. In command current prediction section, the command current $i_c^*(k+2)$ is predicted by using harmonic current $i_c^*(k)$ of load in the current sampling period. The command output voltage $u_o^*(k)$ is calculated by deadbeat control strategy, and switching signals are generated by SPWM section. PI controller could stabilize the DC side voltage, it outputs the control current $i_{\Delta p}(k)$, which is added to the harmonic current extraction section.

III. OPTIMIZATION OF COMMAND CURRENT REPETITIVE PREDICTION

A. LIMITATIONS OF TRADITIONAL COMMAND CURRENT REPETITIVE PREDICTION ALGORITHM

When nonlinear load is under steady state, harmonic current $i_c^*(k)$, predicted current $i_c^*(k+2)$ and the error between $i_c^*(k+2)$ and the actual harmonic current at $(k+2)T_s$ will be periodic. Therefore, repetitive control can be adopted to eliminate this error. The structure of harmonic current extraction and command current repetitive prediction algorithm in abc coordinate system can be seen in Fig. 3 [29], [19].

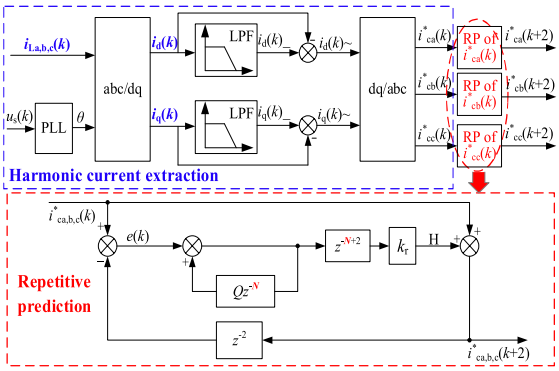

FIGURE 3. Structure of harmonic current extraction and command current repetitive prediction in abc coordinate system.

Repetitive prediction is composed of error accumulation and lead compensation. Prediction error $e(k)$ is sent into error accumulation, after the lead compensation, a correction component H is calculated and added to the harmonic current $i_c^*(k)$ two sampling periods in advance to make the prediction result $i_c^*(k+2)$ close to the actual value.

For the traditional command current repetitive prediction applied in APF, the error accumulation period is the lowest common multiple of each harmonic component's period of load current. That is to say, the error accumulation period is the lowest common multiple of $1/(m \times 50)$ (m is the order of harmonic component in load current). According to this principle, the error accumulation period in abc coordinate system is one power grid cycle (20ms), which indicates that $i_c^*(k+2)$ is corrected by H after 20ms. Therefore, in Fig. 3, N is the number of sampling points in one error accumulation period, in other words, N is the quotient of error accumulation period divided by T_s. In addition, Q and k_r are constant gain less than 1 to ensure the stability of prediction.

After analysis above, conclusions can be obtained as following. On the one hand, the prediction value is corrected

only once in one power grid cycle, which causes the prediction deviation to a certain extent. On the other hand, because N is determined under the assumption that the grid frequency is 50 Hz, prediction accuracy will decline as soon as grid frequency deviates from 50 Hz. Therefore, N needs to be adjusted in real time to track grid frequency fluctuation.

B. FAST REPETITIVE PREDICTION ALGORITHM OF COMMAND CURRENT AGAINST GRID FREQUENCY FLUCTUATION

As Fig. 3, a harmonic current extraction based on abc/dq transformation is applied. For three-phase three-wire system, there is not 3 and its integral multiples order harmonic current. In addition, even-order harmonics are not considered in such system. For the above-mentioned reasons, the order of harmonic components of nonlinear load is $6k\pm1$ ($k = 1,2,3\ldots$) [30].

According to [31], for the n-order positive sequence current, after abc/dq transformation, the order of components on d and q axes will become (n-1). In the same way, for the n-order negative sequence current, after the transformation, the order of components on d and q axes will become ($n+1$).

From the analysis above, in three-phase three-wire system, n-order($n \in 6k\pm1$) harmonic component will be converted to even-order after abc/dq transformation. The frequency correspondence between abc and dq coordinate system is shown in Table 1.

TABLE 1. Frequency correspondence between abc and dq coordinate system.

Frequency of dq (order)	Frequency of abc positive sequence (order)	Frequency of abc negative sequence (order)
0Hz	50Hz(1 order)	-
100Hz(2 order)	-	50Hz(1 order)
200Hz(4 order)	250Hz(5 order)	-
300Hz(6 order)	350Hz(7 order)	250Hz(5 order)
400Hz(8 order)	-	350Hz(7 order)
500Hz(10 order)	550Hz(11 order)	-
600Hz(12 order)	650Hz(13 order)	550Hz(11 order)
700Hz(14 order)	-	650Hz(13 order)

Therefore, the error accumulation period will be reduced to half if repetitive prediction is transferred to dq coordinate system. Meanwhile, N will be reduced to $N/2$, so that the prediction value could be corrected twice in one power grid cycle, which makes the proposed prediction algorithm achieve higher prediction accuracy than the traditional one. That is to say, the correction speed for prediction value becomes faster. The structure of the proposed fast repetitive prediction algorithm is shown as Fig. 4.

In addition, when grid frequency fluctuates, $N/2$ may not be an integer, given:

$$\frac{N}{2} \approx \left[\frac{N}{2} - \frac{l}{2}\right] + \left(\frac{N}{2} - \left[\frac{N}{2} - \frac{l}{2}\right]\right) = N_{\mathrm{I}} + N_{\mathrm{F}} \tag{7}$$

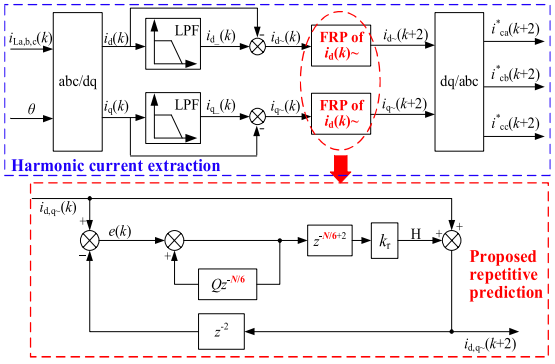

FIGURE 4. Structure of harmonic current extraction and the proposed fast repetitive prediction.

where N_{I} is the integer closest to $(N/2 - l/2)$, and l is the approximate order of the fractional part N_{F} [32].

The fractional part N_{F} can be expressed approximatively by Lagrange interpolation polynomial:

$$z^{-N_{\mathrm{F}}} \approx \sum_{n=0}^{l} f(n) z^{-n} \tag{8}$$

where $f(n)$ is coefficient for the equivalent integral delay beat z^{-n}, which can be seen in (9) [33].

$$f(n) = \prod_{n=0, n\neq n}^{l} \frac{N_{\mathrm{F}} - m}{n - m} \tag{9}$$

For example, when l is set to 2, the coefficients are as follows:

$$\begin{cases} f(0) = (N_{\mathrm{F}} - 1)(N_{\mathrm{F}} - 2)/2 \\ f(1) = -N_{\mathrm{F}}(N_{\mathrm{F}} - 2) \\ f(2) = N_{\mathrm{F}}(N_{\mathrm{F}} - 1)/2 \end{cases} \tag{10}$$

After the decomposition and equivalence for $N/2$, when grid frequency fluctuates, the integral delay beat number N_{I} could be adjusted adaptively, and the fractional delay beat number N_{F} could be converted to integer. Therefore, the proposed prediction algorithm will adapt to grid frequency fluctuation. The structure of the fast command current repetitive prediction algorithm against grid frequency fluctuation is shown in Fig. 5.

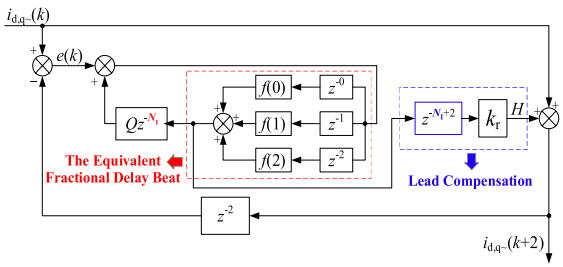

FIGURE 5. Structure of the fast repetitive prediction algorithm against frequency fluctuation in dq coordinate system.

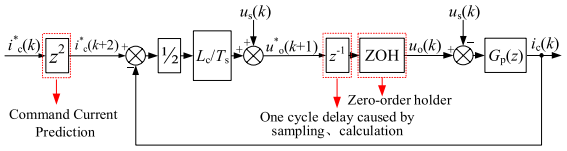

FIGURE 6. Block diagram of traditional deadbeat control in current inner loop of APF.

IV. IMPROVEMENT OF DEADBEAT CONTROL STRATEGY FOR CURRENT TRACKING

A. LIMITATIONS OF TRADITIONAL DEADBEAT CONTROL STRATEGY

According to section II, the command voltage of traditional deadbeat can be calculated by (6).

However, the corresponding control system is not stable, for the purpose of stabilizing the system and obtaining a margin, a gain less than 1 is usually introduced into the control channel, which is generally set to 1/2 [21], [23]. Therefore, in practical application for traditional deadbeat control strategy, the command voltage can be obtained by (11), and the corresponding control block diagram is shown in Fig. 6.

$$u_o^*(k+1) = \frac{L_c}{2T_s}\left[i_c^*(k+2) - i_c(k)\right] + u_s(k) \tag{11}$$

where $G_p(z)$ is discrete transfer function of the controlled object (L_c).

$$G_p(z) = \frac{T_s}{L_c(z-1)} \tag{12}$$

By calculating (2) backward for one sampling period, (13) could be obtained:

$$i_c(k+2) = i_c(k+1) + \frac{T_s}{L_c}\left[u_o(k+1) - u_s(k+1)\right] \tag{13}$$

(14) will be gotten if introduce $i_c(k+2) = i_c^*(k+2)$ into (13).

$$i_c^*(k+2) = i_c(k+1) + \frac{T_s}{L_c}\left[u_o^*(k+1) - u_s(k+1)\right] \tag{14}$$

In current sampling period $kT_s - (k+1)T_s$, if the actual output current $i_c(k+1)$ can be estimated, the output voltage command $u_o^*(k+1)$ operating in next sampling period $(k+1)T_s - (k+2)T_s$ will be calculated through (14). Under this condition, $i_c(k+2)$ can track $i_c^*(k+2)$ through $u_{ox}^*(k+1)$, and the tracking performance depends on the estimation accuracy of $i_c(k+1)$.

In traditional deadbeat control strategy, from the comparison of (11) and (14), it can be known t2hat $i_c(k+1)$ do not be predicted at $(k+1)T_s$, but is replaced by the output current sampled at kT_s ($i_c(k)$). Moreover, the introduction of the gain of 1/2 reduces tracking capability further. To deal with this problem, an improved deadbeat control strategy is proposed in this article, which estimates the output current at $(k+1)T_s$ in current sampling period $kT_s - (k+1)T_s$, so as to strengthen the harmonic compensation performance of APF.

B. THE IMPROVED DEADBEAT CONTROL STRATEGY

By calculating (2) forward for one sampling period, (15) will be derived:

$$i_c(k) = i_c(k-1) + \frac{T_s}{L_c}\left[u_o(k-1) - u_s(k-1)\right] \tag{15}$$

Based on (2) and (15), $i_c(k+1)$ sampled at the moment of $(k+1)T_s$ can be expressed as (16)

$$i_c(k+1) = 2i_c(k) - i_c(k-1) + \frac{T_s}{L_c}\left[u_o(k) - u_o(k-1) - u_s(k) + u_s(k-1)\right] \tag{16}$$

In SPWM, on account of a modulation delay of half sampling period from the loading of modulation signal (command voltage) to the output of corresponding switching signals, half a period will be taken for the conversion of command voltage $u_o^*(k)$ to actual voltage $u_{ox}(k)$ [34], [35].

The modulation process of SPWM can be represented by zero order holder (ZOH), the transfer function of ZOH is described as (17).

$$\mathrm{ZOH}(z) = z^{-0.5} \approx \frac{1}{2}(z^{-1}+1) \tag{17}$$

Then the actual output voltage of APF at $(k-1)T_s$ and kT_s can be approximately estimated as (18) and (19).

$$\tilde{u}_o(k) \approx \frac{1}{2}\left[u_o^*(k) + u_o^*(k-1)\right] \tag{18}$$

$$\tilde{u}_o(k-1) \approx \frac{1}{2}\left[u_o^*(k-1) + u_o^*(k-2)\right] \tag{19}$$

The estimated value of output current $\tilde{i}_c(k+1)$ at $(k+1)T_s$ can be calculated by introducing (18), (19) into (17), which is shown in (20).

$$\tilde{i}_c(k+1) = 2i_c(k) - i_c(k-1) + \frac{T_s}{L_c}\left[\tilde{u}_o(k) - \tilde{u}_o(k-1) - u_s(k) + u_s(k-1)\right] \tag{20}$$

Based on the deduction above, the improved calculation formula for command voltage could be obtained by introducing the estimation expression (20) into (15):

$$u_o^*(k+1) = \frac{L_c}{T_s}\left[i_c^*(k+2) - (2i_c(k) - i_c(k-1))\right] - \left[\frac{1}{2}(u_o^*(k) - u_o^*(k-2)) + u_s(k-1) - u_s(k) - u_s(k+1)\right] \tag{21}$$

Fig. 7. shows the block diagram of the improved deadbeat control in discrete domain.

From Fig. 6, closed-loop transfer function of traditional deadbeat control can be expressed as (22).

$$G_{\mathrm{conDBC}}(z) = \frac{z^2(z+1)}{4z^3 - 4z^2 + z + 1} \tag{22}$$

Closed-loop transfer function of the improved deadbeat control can be obtained from Fig. 7, as (23).

$$G_{\mathrm{impDBC}}(z) = \frac{z(z+1)}{2z^2 - z + 1} \tag{23}$$

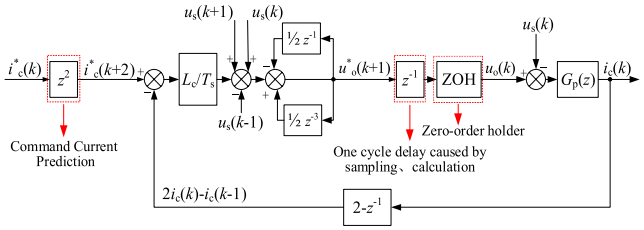

FIGURE 7. Block diagram of the improved deadbeat control strategy incurrent inner loop.

According to (22) and (23), the zero-pole distribution of $G_{\text{conDBC}}(z)$ and $G_{\text{impDBC}}(z)$ is shown in Fig. 8.

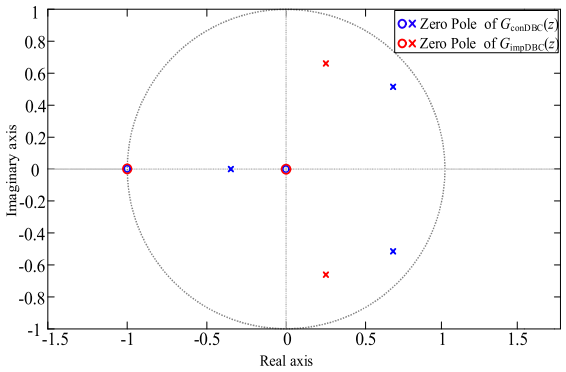

FIGURE 8. Zero-pole distribution of $G_{\text{conDBC}}(z)$ and $G_{\text{impDBC}}(z)$.

It can be inferred from Fig. 8 that all of the poles of the improved control system are contained by the unit circle, which proves that the improved control system is stable. Take this as the premise, the Bode diagram of $G_{\text{conDBC}}(z)$, $G_{\text{impDBC}}(z)$ can be obtained as shown in Fig. 9.

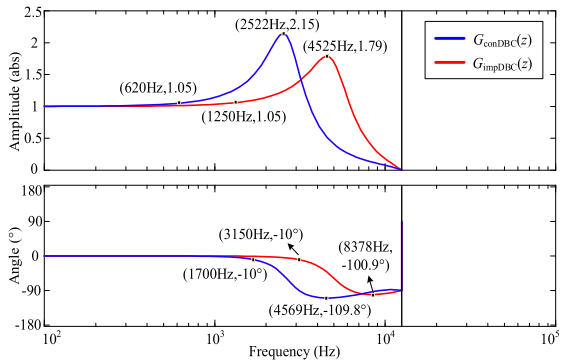

FIGURE 9. Bode diagram of $G_{\text{conDBC}}(z)$ and $G_{\text{impDBC}}(z)$.

From the upper part of Fig. 9, when frequency is 620Hz, a gain exceeding 1 (1.05) which corresponds to the overcompensation phenomenon could be found in the output current using traditional deadbeat control strategy. Under the same conditions, the corresponding frequency of the improved deadbeat control could be extended to 1250Hz. In the down part of Fig. 9, with traditional deadbeat control, a phase lag of 10° in the output current could be observed at frequency of 1700Hz, while the corresponding frequency of the improved control could increase to 3150Hz under the same condition. Therefore, the harmonic compensation performance of the improved deadbeat control system is better than the traditional one within the range of 0-1250Hz, in other words, the effective controlled frequency band of the control system is enlarged.

C. ERROR REPETITIVE CORRECTION BASED ON THE IMPROVED DEADBEAT CONTROL STRATEGY

Considering that the current tracking error $i(k) - i^*(k)$ changes periodically in steady state, the tracking error in the previous power grid cycle can be set as a correction value to add into the control channel of the improved control system in current power grid cycle. In this way, an error repetitive correction based on the improved deadbeat control strategy is formulated, which can reduce the periodic current tracking error to a certain extent. The control structure diagram can be seen in Fig. 10.

In Fig. 10, $E(z)$ is the current tracking error, k_{RC} is a gain of the error repetitive correction section, and M is the number of delay beats for one power grid cycle (M = power grid cycle /T_s). $G_{\text{R-E}}(z)$ is defined as the transfer function from command signal $R(z)$ to tracking error signal $E(z)$, then $E(z)$ can be described by (24).

$$\begin{aligned} E(z) &= G_{\text{R-E}}(z)R(z) \\ &= \frac{1 + H(z)G_p(z)G_c(z) - z^2G_p(z)G_c(z)}{1 + H(z)G_p(z)G_c(z) + G_p(z)G_c(z)G_{RC}(z)}R(z) \end{aligned} \quad (24)$$

The characteristic equation of $G_{\text{R-E}}(z)$ is:

$$1 + H(z)G_p(z)G_c(z) + G_p(z)G_c(z)G_{RC}(z) = 0 \quad (25)$$

It has been proved above that the control system without error repetitive correction is stable. Therefore, the sufficient and necessary condition for system stability is that all the eigenvalues are in unit circle. Specific characteristic equation of $G_{\text{R-E}}(z)$ can be gotten by introducing $G_{\text{p}}(z)$, $G_{\text{c}}(z)$, $H(z)$, and $G_{\text{RC}}(z)$ into (25), as (26).

$$\left[k_{\text{RC}}z^{-N}(z+1) + 2z^3 - z^2 + z\right]z = 0 \quad (26)$$

This is an equation about z, where one of the solutions is $z = 0$, then the remaining solutions could be described by (27).

$$k_{\text{RC}}z^{-N}(z+1) + 2z^3 - z^2 + z = 0 \quad (27)$$

From the deformation of (27), z is expressed as (28).

$$z = \sqrt[N+1]{\frac{(z+1)k_{RC}}{-2z^2 + z - 1}} = \sqrt[N+1]{T(z)k_{RC}} \quad (28)$$

If $|T(z)k_{RC}| < 1$, there must be $|z| < 1$, thus a sufficient condition for system stability is $|T(z)k_{RC}| < 1$.

In order to find the maximum of $|T(z)|$ which can ensure absolute stability of the control system, the Nyquist diagram of $T(z)$ is drawn in Fig. 11.

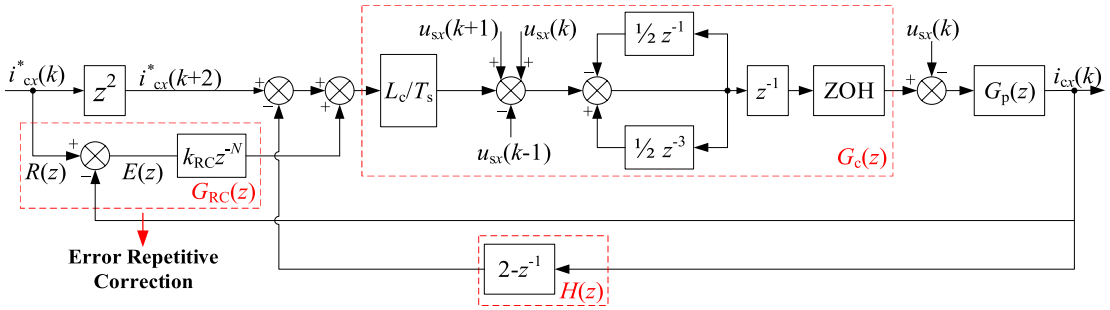

FIGURE 10. Block diagram of the improved deadbeat control combined with the error repetitive correction in current inner loop.

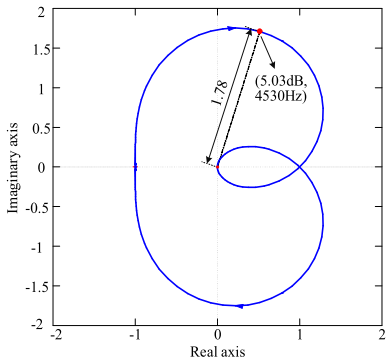

FIGURE 11. Nyquist curve of $T(z)$.

The maximum amplitude of $T(z)$ is about 1.78 (5.03dB) at the frequency of 4530Hz, thus the sufficient condition for system stability is:

$$1.78k_{RC} < 1 \tag{29}$$

Consequently, the reasonable range of k_{RC} is [0, 0.56).

$G_{R-E}(z)$ reflects the control system's tracking performance for the command current. The amplitude-frequency characteristic curves of $G_{R-E}(z)$ are drawn in Fig. 12, when k_{RC} is 0, 0.15, 0.3 and 0.45 respectively.

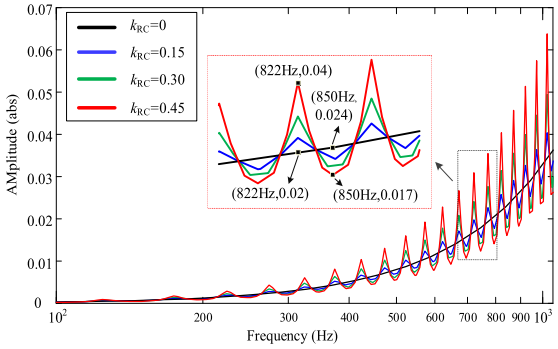

FIGURE 12. Amplitude-frequency characteristic curve of $G_{R-E}(z)$ with different values of k_{RC}.

From Fig. 12, when $k_{RC} \neq 0$, the obvious "depressions" can be seen in the amplitude frequency characteristics of $G_{R-E}(z)$ at the fundamental and its integral multiple frequency, that is, the steady-state tracking error $E(z)$ of the control system is smaller than that without error repetitive correction ($k_{RC} = 0$) at these frequencies. The control system could obtain better tracking performance for command current. At the same time, with the increase of k_{RC}(but not more than 0.56), the harmonic compensation performance of APF will be obviously enhanced.

V. SIMULATION AND EXPERIMENT VERIFICATION

For verifying the effectiveness of the proposed repetitive prediction algorithm for command current and the improved deadbeat control strategy for current inner loop in this article, a simulation model and a HIL experimental platform are built in accordance with the grid-connected three phase APF system structure shown in Fig. 1.

The simulation model is built by Matlab/Simulink toolbox. The HIL experimental platform is established with the real-time digital simulator opal-rt 5600 as controller, IGBT as the power electronic switching device (the type is 2SP0115T: including IGBT and its driving module), a DC power supply as the DC-side bus (the type is N5771A 300V/5A,1500W).

The nonlinear load is three-phase uncontrolled rectifier with resistor on DC side. Simulation and experiment parameters are shown in Table 2 and Table 3 respectively. The overall experimental platform is shown in Fig. 13.

TABLE 2. Simulation parameters.

Parameters	Value
Three-phase power line voltage U_{sl}/V	380
Rated frequency of power grid f_N/Hz	50
AC-side inductance L_c/mH	1.3
DC side capacitance C_{dc}/μF	1000
DC side voltage U_{dc}/V	800
Load resistance R_L/Ω	10
Distortion rate of load current THD/%	25.22
Control system sampling frequency f_s/kHz	25

A. SIMULATION VERIFICATION FOR THE FAST REPETITIVE PREDICTION ALGORITHM OF COMMAND CURRENT AGAINST GRID FREQUENCY FLUCTUATION

For the purpose of verifying effectiveness of the proposed prediction algorithm, the traditional and proposed prediction

TABLE 3. Experiment parameters.

Parameters	Value
Three-phase power line voltage U_{sl}/V	50
Rated frequency of power grid f_N/Hz	50
AC-side inductance L_c/mH	1.3
DC side voltage U_{dc}/V	120
Load resistance R_L/Ω	5
Distortion rate of load current THD/%	24.18
Control system sampling frequency f_s/kHz	25

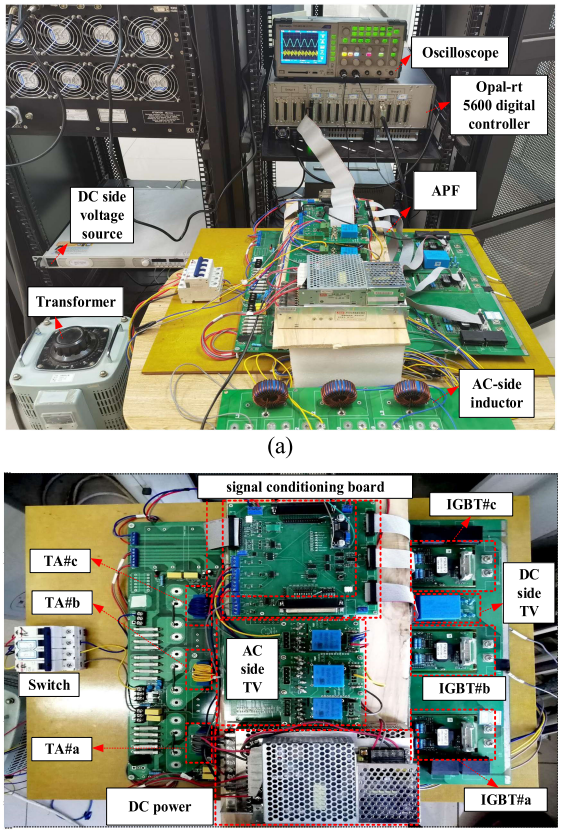

FIGURE 13. Experimental platform in laboratory. (a) Overall hardware platform of APF system. (b) Power board and signal conditioning board.

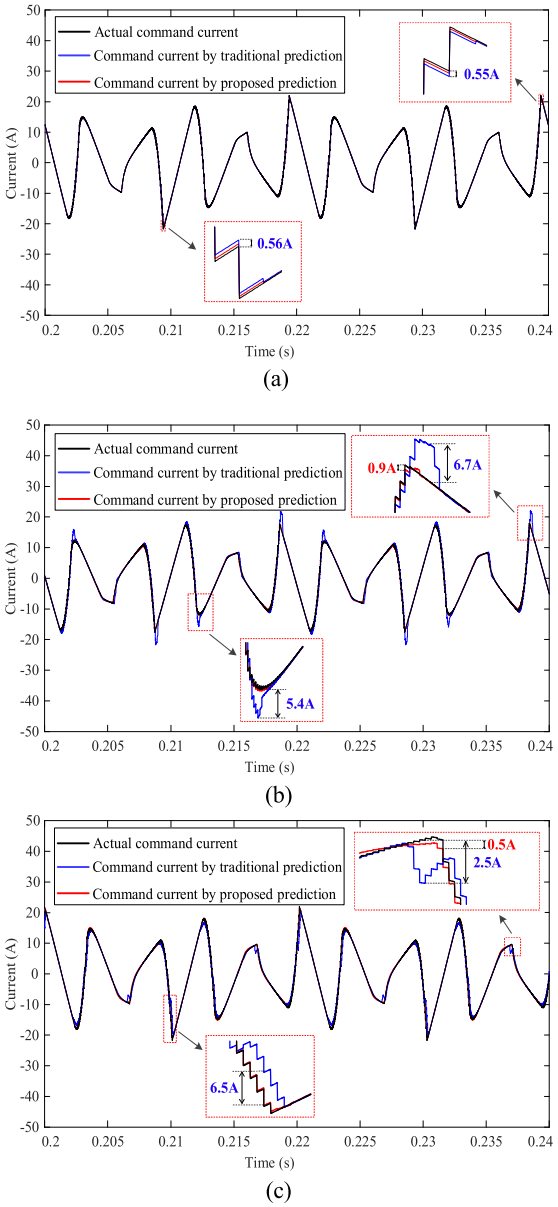

FIGURE 14. Predicted command current with traditional or proposed prediction algorithm at different grid frequency. (a) Grid frequency of 50Hz. (b) Grid frequency of 50.5Hz. (c) Grid frequency of 49.5Hz.

algorithms are adopted to predict the command current at grid frequency of 50Hz, 50.5Hz, and 49.5Hz. The simulation results can be seen in Fig. 14 (a), (b) and (c).

In Fig. 14(a), when grid frequency is 50Hz, there exists a small prediction deviation by the traditional prediction algorithm, while the predicted value $i_c^*(k+2)$ of the proposed prediction algorithm is essentially coincident with the actual command current. This result indicates that the prediction accuracy of command current could be increased to a certain extent by transferring the repetitive prediction from abc to dq coordinate system.

Besides, in Fig. 14(b) and (c), when grid frequency deviates from 50Hz (50.5Hz, 49.5Hz), there exists obvious prediction error with the traditional algorithm (the maximum prediction error is about 6.7A), while the prediction error of the proposed prediction algorithm is decreased obviously (the maximum prediction error is only 0.9A). Therefore, the proposed prediction algorithm has strong adaptability to grid frequency fluctuation.

B. SIMULATION VERIFICATION FOR THE IMPROVED DEADBEAT CONTROL STRATEGY WITH PROPOSED PREDICTION ALGORITHM

To investigate the APF harmonic compensation performance under grid frequency fluctuation conditions, the improved

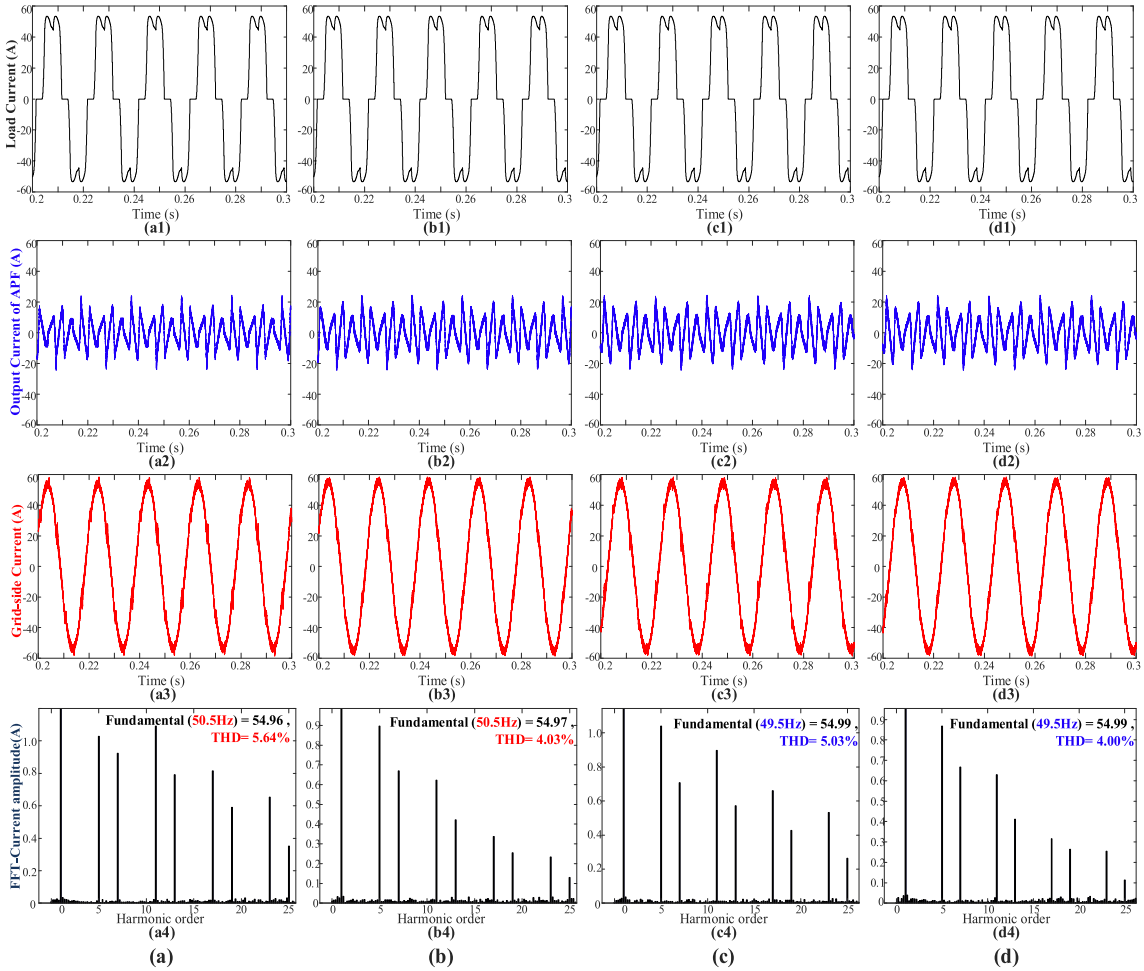

FIGURE 15. Simulation results for the improved deadbeat control strategy with traditional or proposed repetitive prediction. (a) With traditional prediction at grid frequency of 50.5Hz. (b) With proposed prediction at grid frequency of 50.5Hz (c) With traditional prediction at grid frequency of 49.5Hz. (d) With proposed prediction at grid frequency of 49.5Hz.

deadbeat control strategy is adopted with traditional and proposed repetitive prediction respectively. Fig.15(a) exhibits simulation result by using traditional repetitive prediction algorithm, and Fig.15(b) corresponds to the proposed repetitive prediction against grid frequency fluctuation when grid frequency is 50.5Hz. Similarly, Fig.15(c) and (d) are the simulation results at grid frequency of 49.5Hz.

In comparison with simulation results of the improved deadbeat control strategy using traditional prediction, the improved deadbeat control strategy using the proposed prediction could reduce the THD of grid-side current from 5.64% (at grid frequency of 50.5Hz), 5.03% (at grid frequency of 49.5Hz) to 4.03%, 4.00%.

Because the proposed prediction algorithm could adapt to grid frequency fluctuation, the improved deadbeat control strategy using the proposed prediction is scarcely influenced by grid frequency fluctuation. Meanwhile, it is indirectly identified that the prediction accuracy of command current is the prerequisite for harmonic compensation performance of deadbeat control strategy.

C. EXPERIMENTAL VERIFICATION FOR THE IMPROVED DEADBEAT CONTROL STRATEGY

According to the parameters in Table 3, a steady-state harmonic compensation experiment is accomplished to investigate the harmonic compensation performance of this APF system with the improved($k_{RC} = 0$) and traditional deadbeat control strategy in inner current loop. The power grid voltage and nonlinear load current are shown in Fig. 16. The grid-side current and APF output current of phase A can be seen in Fig. 17. Moreover, fundamental and harmonic components of grid-side current are counted by the harmonic analysis module of oscilloscope in Fig. 17.

In Fig.17, compared with traditional deadbeat control strategy, when the improved deadbeat is applied, harmonic compensation performance of APF is improved significantly. Specifically, it has a better compensation effect within the range of 0-1250Hz with the improved deadbeat strategy.

Furthermore, harmonic compensation experiment is carried out with the improved deadbeat-error repetitive correction control strategy (k_{RC} is 0.15, 0.3, 0.45 respectively).

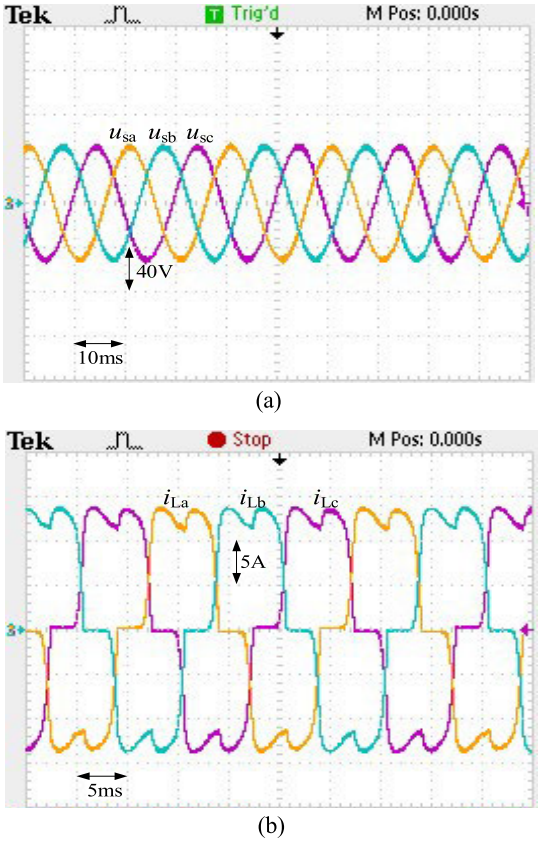

FIGURE 16. Power grid voltage and nonlinear load current. (a) Power grid voltage. (b) Nonlinear load current.

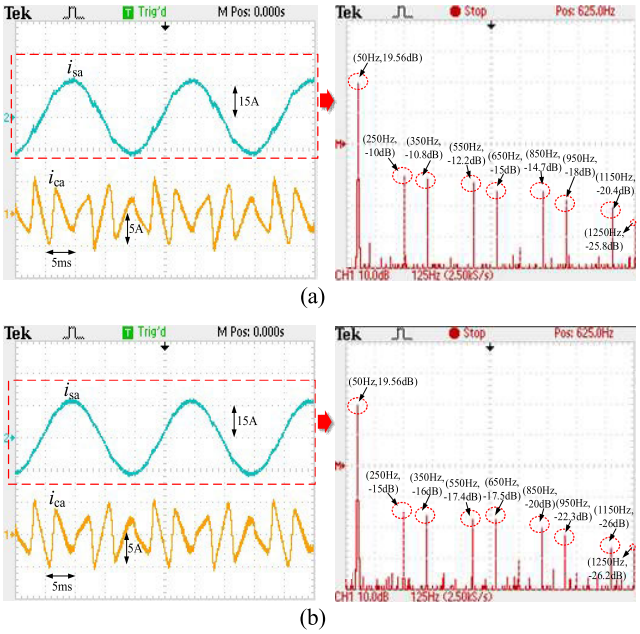

FIGURE 17. Grid-side current and output current of phase A with traditional or improved deadbeat control strategy. (a) Traditional deadbeat. (b) Improved deadbeat ($k_{RC} = 0$).

The grid-side current and output current of phase A (as well as harmonic analysis) can be seen in Fig.18.

For the purpose of quantitative analysis of APF harmonic compensation effect with different k_{RC}, based on the

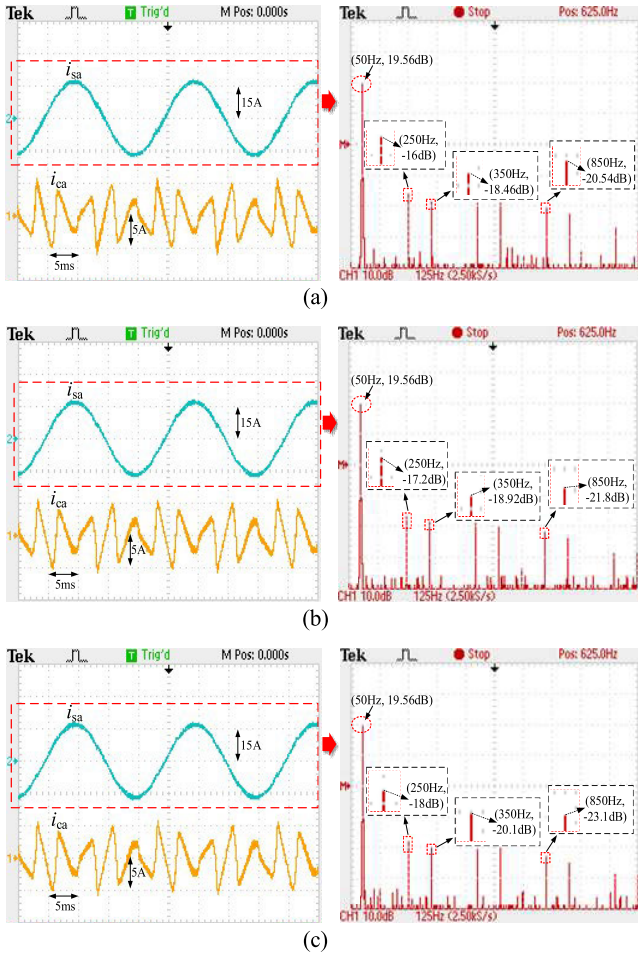

FIGURE 18. Grid-side current and output current of phase A with different value of k_{RC}. (a) $k_{RC} = 0.15$. (b) $k_{RC} = 0.30$. (c) $k_{RC} = 0.45$.

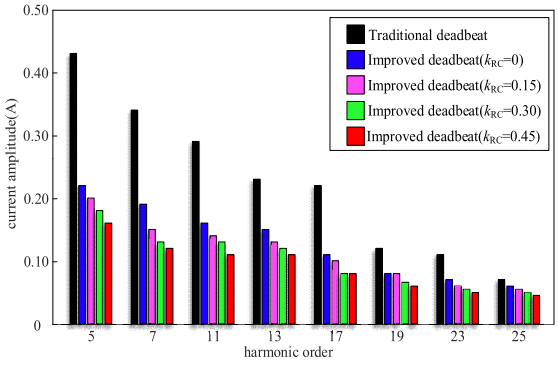

FIGURE 19. Characteristic harmonic components of grid-side current with different control strategies.

harmonic analysis results, the comparison of characteristic harmonic components under different control strategies is shown in Fig. 19. Moreover, the total harmonic distortion of grid-side current can be seen in Table 4.

From Table 4 and Fig.17-19, when the error repetitive correction is added into the improved deadbeat control channel, the harmonic compensation capability of APF could also get enhanced to a certain extent with the increase of k_{RC}

TABLE 4. Total harmonic distortion of grid-side current with different control strategies.

Control strategy and parameters	Total harmonic distortion of grid-side current
Traditional deadbeat control strategy	5.45%
Improved deadbeat control strategy (k_{RC}=0)	3.81%
Improved deadbeat-error repetitive correction control strategy (k_{RC}=0.15)	3.68%
Improved deadbeat-error repetitive correction control strategy (k_{RC}=0.30)	3.57%
Improved deadbeat-error repetitive correction control strategy (k_{RC}=0.45)	3.50%

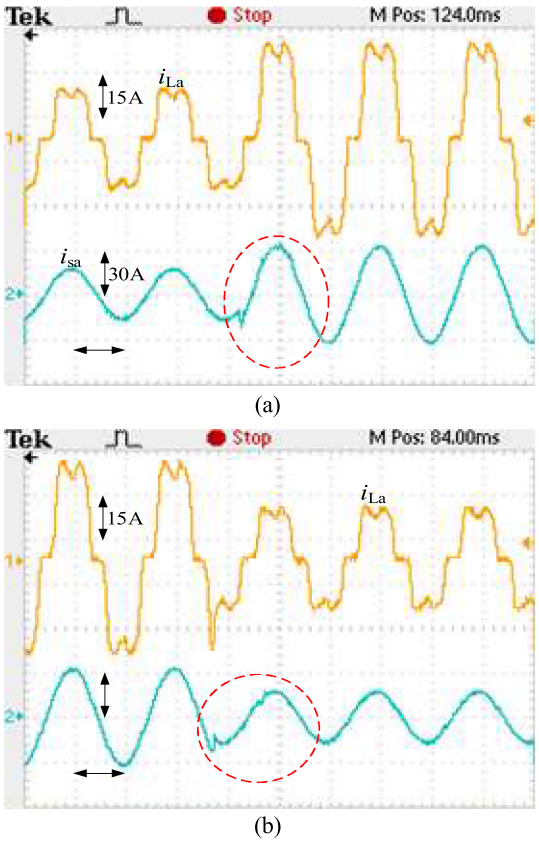

FIGURE 20. Simulation results for dynamic-state harmonic compensation using the proposed control method. (a) With the increase of load current. (b) With the decrease of load current.

Finally, for revealing the superiority of the improved deadbeat control strategy comprehensively, the verification for dynamic response of the improved control strategy is realized by changing the load resistance R_L. R_L decreases from 5Ω to 2.5Ω (for increase in load current) or increases from 2.5Ω to 5Ω (for decrease in load current). The simulation results are shown in Fig. 20.

In Fig.20, when the load current increases or decreases, there is a transient process lasting less than 1/2 power grid cycle. So the satisfactory dynamic-state harmonic compensation performance of the proposed control method can be indicated.

VI. CONCLUSION

In order to improve the harmonic compensation performance of APF, command current prediction algorithm and deadbeat control strategy for current tracking are optimized in this article. The feasibility and effectiveness of the proposed method are verified by theoretical analysis, simulation, and experiment. The conclusions are as follows:

(1) The accuracy of command current prediction is the prerequisite for optimizing the current tracking control strategy. Compared with the traditional command current repetitive prediction algorithm, the proposed one exhibits higher prediction accuracy and stronger adaptability to the fluctuation of grid frequency.

(2) Compared with the traditional deadbeat control, because the APF output current in the next sampling period has been estimated, the effective controlled frequency band of the control system is enlarged on the premise of ensuring system stability.

(3) When current tracking error repetitive correction is added into the improved deadbeat control channel, the periodic tracking error could be reduced to some extent, and the control accuracy is increased as well.

(4) The simulation and experiment results demonstrate that the proposed control method has a fine steady-state performance to grid frequency fluctuation and a satisfactory dynamic response to the sudden change of load current.

REFERENCES

[1] Y. Fang, J. Fei, and T. Wang, "Adaptive backstepping fuzzy neural controller based on fuzzy sliding mode of active power filter," *IEEE Access*, vol. 8, pp. 96027–96035, Jun. 2020.
[2] J. Chen, H. Shao, Y. Cheng, X. Wang, G. Li, and C. Sun, "Harmonic circulation and DC voltage instability mechanism of parallel-SVG system," *IET Renew. Power Gener.*, vol. 14, no. 5, pp. 793–802, Apr. 2020.
[3] J. Fei and Y. Chu, "Double hidden layer output feedback neural adaptive global sliding mode control of active power filter," *IEEE Trans. Power Electron.*, vol. 35, no. 3, pp. 3069–3084, Mar. 2020.
[4] W. U. K. Tareen and S. Mekhielf, "Three-phase transformerless shunt active power filter with reduced switch count for harmonic compensation in grid-connected applications," *IEEE Trans. Power Electron.*, vol. 33, no. 6, pp. 4868–4881, Jun. 2018.
[5] Z.-X. Zou, K. Zhou, Z. Wang, and M. Cheng, "Frequency-adaptive fractional-order repetitive control of shunt active power filters," *IEEE Trans. Ind. Electron.*, vol. 62, no. 3, pp. 1659–1668, Mar. 2015.
[6] B. L. G. Costa, V. D. Bacon, S. A. O. da Silva, and B. A. Angelico, "Tuning of a PI-MR controller based on differential evolution Metaheuristic applied to the current control loop of a shunt-APF," *IEEE Trans. Ind. Electron.*, vol. 64, no. 6, pp. 4751–4761, Jun. 2017.
[7] S. Buso, L. Malesani, and P. Mattavelli, "Comparison of current control techniques for active filter applications," *IEEE Trans. Ind. Electron.*, vol. 45, no. 5, pp. 722–729, Oct. 1998.
[8] C.-S. Lam, Y.-D. Han, and M.-C. Wong, "Hysteresis current control of hybrid active power filters," *IET Power Electron.*, vol. 5, no. 7, pp. 1175–1187, Aug. 2012.
[9] S. R. Angadi, R. Nanjundaswamy, N. R. Srinivas, and R. S. Ananda Murthy, "A hysteresis current control based shunt current compensation scheme for power quality improvement in high power radiology applications," in *Proc. Int. Conf. Power Adv. Control Eng. (ICPACE)*, Bangalore, India, Aug. 2015, pp. 53–58.

[10] J. Allmeling, "A control structure for fast harmonics compensation in active filters," *IEEE Trans. Power Electron.*, vol. 19, no. 2, pp. 508–514, Mar. 2004.
[11] V. D. Bacon and S. A. O. da Silva, "Selective harmonic currents suppressing applied to a three-phase shunt active power filter based on adaptive filters," in *Proc. IEEE 13th Brazilian Power Electron. Conf. 1st Southern Power Electron. Conf. (COBEP/SPEC)*, Fortaleza, Brazil, Nov. 2015, pp. 1–6.
[12] G. Pandove and M. Singh, "Robust repetitive control design for a three-phase four wire shunt active power filter," *IEEE Trans. Ind. Informat.*, vol. 15, no. 5, pp. 2810–2818, May 2019.
[13] L. He, K. Zhang, J. Xiong, and S. Fan, "A repetitive control scheme for harmonic suppression of circulating current in modular multilevel converters," *IEEE Trans. Power Electron.*, vol. 30, no. 1, pp. 471–481, Jan. 2015.
[14] S. Yang, P. Wang, Y. Tang, and L. Zhang, "Explicit phase lead filter design in repetitive control for voltage harmonic mitigation of VSI-based islanded microgrids," *IEEE Trans. Ind. Electron.*, vol. 64, no. 1, pp. 817–826, Jan. 2017.
[15] W. Jiang, W. Ma, J. Wang, L. Wang, and Y. Gao, "Deadbeat control based on current predictive calibration for grid-connected converter under unbalanced grid voltage," *IEEE Trans. Ind. Electron.*, vol. 64, no. 7, pp. 5479–5491, Jul. 2017.
[16] B. Wang, U. Manandhar, X. Zhang, H. B. Gooi, and A. Ukil, "Deadbeat control for hybrid energy storage systems in DC microgrids," *IEEE Trans. Sustain. Energy*, vol. 10, no. 4, pp. 1867–1877, Oct. 2019.
[17] L. Shi, R. Cai, L. Chen, and P. Wang, "A deadbeat control scheme for three-phase three-wire active power filter," *Power Syst. Protection Control*, vol. 42, no. 14, pp. 32–37, Jul. 2014.
[18] Y. Han, C. Zhan, L. Zhao, and M. Wong, "Control of tri-level shunt power quality conditioners," *J. Tsinghua Univ.*, vol. 40, no. 3, pp. 40–43, Mar. 2000.
[19] Y. He, J. Liu, J. Tang, Z. Wang, and Y. Zou, "Deadbeat control with a repetitive predictor for three-level active power filters," *J. Power Electron.*, vol. 11, no. 4, pp. 583–590, Jul. 2011.
[20] X. Chen, T. Wang, H. Wang, Y. Hou, and L. Guo, "A magnetic flux compensated series active power filter using deadbeat control based on repetitive predictor theory," in *Proc. 22nd Int. Conf. Electr. Mach. Syst. (ICEMS)*, Harbin, China, Aug. 2019, pp. 1–5.
[21] L. Y. Yang, S. Yang, W. P. Zhang, Z. G. Chen, and L. Xu, "The improved deadbeat predictive current control method for single-phase PWM rectifiers," *Proc. CSEE*, vol. 35, no. 22, pp. 5842–5850, Nov. 2015.
[22] W. Jiang, X. Ding, Y. Ni, J. Wang, L. Wang, and W. Ma, "An improved deadbeat control for a three-phase three-line active power filter with current-tracking error compensation," *IEEE Trans. Power Electron.*, vol. 33, no. 3, pp. 2061–2072, Mar. 2018.
[23] Y. Liang, J. Liu, and Z. Li, "Improved deadbeat-repetitive control strategy for active power filter," *Trans. China Electrotech. Soc.*, vol. 33, no. 19, pp. 4573–4582, Oct. 2018.
[24] D. Li, X. Kong, and L. Liu, "Deadbeat and fast repetitive control for single-phase dual-buck inverter," *Power Syst. Technol.*, vol. 43, no. 10, pp. 3671–3677, Oct. 2019.
[25] H. Chen, B. Sun, J. Qu, and K. Fu, "An improved deadbeat control strategy for D-STATCOM based on frequency-adaptive repetitive predictor," in *Proc. IEEE Int. Conf. Cyber Technol. Autom., Control, Intell. Syst. (CYBER)*, Shenyang, China, Jun. 2015, pp. 1720–1725.
[26] A. Lidozzi, C. Ji, L. Solero, P. Zanchetta, and F. Crescimbini, "Digital deadbeat and repetitive combined control for a stand-alone four-leg VSI," *IEEE Trans. Ind. Appl.*, vol. 53, no. 6, pp. 5624–5633, Nov. 2017.
[27] C. Tan, Q. Chen, K. Zhou, and L. Zhang, "A simple high-performance current control strategy for V2G three-phase four-leg inverter with LCL filter," *IEEE Trans. Transp. Electrific.*, vol. 5, no. 3, pp. 695–701, Sep. 2019.
[28] S. Bosch, J. Staiger, and H. Steinhart, "Predictive current control for an active power filter with LCL-filter," *IEEE Trans. Ind. Electron.*, vol. 65, no. 6, pp. 4943–4952, Jun. 2018.
[29] Q. Yan, X. Wu, X. Yuan, and Y. Geng, "An improved grid-voltage feedforward strategy for high-power three-phase grid-connected inverters based on the simplified repetitive predictor," *IEEE Trans. Power Electron.*, vol. 31, no. 5, pp. 3880–3897, May 2016.
[30] W. Lu, K. Zhou, M. Cheng, and Y. Yang, "A novel 6k±1 order harmonic repetitive control scheme for CVCF three-phase PWM inverters," in *Proc. Int. Conf. Elect. Mach. Syst.*, Beijing, China, Aug. 2011, pp. 1–4.
[31] C. Sun, G. Wei, and Z. Bi, "Detection for reactive and harmonics currents of unbalanced three-phase systems based on synchronous reference frame transformation," *Proc. CSEE*, vol. 23, no. 12, pp. 43–48, Dec. 2003.
[32] H. Geng, Z. Zheng, T. Zou, B. Chu, and A. Chandra, "Fast repetitive control with harmonic correction loops for shunt active power filter applied in weak grid," *IEEE Trans. Ind. Appl.*, vol. 55, no. 3, pp. 3198–3206, May 2019.
[33] Z. Liu, B. Zhang, and K. Zhou, "Universal fractional-order design of linear phase lead compensation multirate repetitive control for PWM inverters," *IEEE Trans. Ind. Electron.*, vol. 64, no. 9, pp. 7132–7140, Sep. 2017.
[34] L. Yang and J. Yang, "A robust dual-loop current control method with a delay-compensation control link for LCL-type shunt active power filters," *IEEE Trans. Power Electron.*, vol. 34, no. 7, pp. 6183–6199, Jul. 2019.
[35] J. Ma, X. Wang, F. Blaabjerg, L. Harnefors, and W. Song, "Accuracy analysis of the zero-order hold model for digital pulse width modulation," *IEEE Trans. Power Electron.*, vol. 33, no. 12, pp. 10826–10834, Dec. 2018.

JIKAI CHEN (Member, IEEE) was born in Shaanxi, China, in 1977. He received the Ph.D. degree in electrical engineering from the Harbin Institute of Technology, Harbin, China, in 2011. He is currently a Professor with the School of Electrical Engineering, Northeast Electric Power University (NEEPU), Jilin, China. His research interests include MMC control technologies, analysis and control of power quality, and modeling analysis and control of power-electronics-dominated power systems.

HUI SHAO was born in Shandong, China, in 1995. He received the B.S. degree from Qufu Normal University, Rizhao, China, in 2018. He is currently pursuing the M.S. degree in electrical engineering with Northeast Electric Power University. His research interests include power quality control and optimization of distribution networks.

CHUANG LIU (Member, IEEE) received the M.S. degree from Northeast Electric Power University, Jilin, China, in 2009, and the Ph.D. degree from the Harbin Institute of Technology, Harbin, China, in 2013, all in electrical engineering. From 2010 to 2012, he was with the Future Energy Electronics Center, Virginia Polytechnic Institute and State University, Blacksburg, VA, USA, as a Visiting Ph.D. Student. In 2016, he has been a Professor with the School of Electrical Engineering, Northeast Electric Power University. His research interests include power-electronics-based transformer and power-electronics-based power system stability analysis and control.